Behavioral/Cognitive

Dopamine Dynamics in the Nucleus Accumbens Reflect Confidence in Detecting the Occurrence and Nonoccurrence of Visual Signals in Perceptual Decision-Making

Livia J. F. Wilod Versprille,[1] Colin McKenzie,[1] Felippe E. Amorim,[1] Koji Yano,[2,3] Jeffrey W. Dalley,[1,4] and Trevor W. Robbins[1]

[1]Department of Psychology, University of Cambridge, Cambridge CB2 3EB, United Kingdom, [2]Shionogi & Co., Ltd., Osaka 530-0011, Japan, [3]Medicine Division, Nippon Boehringer Ingelheim Co., Ltd., Tokyo 141-6017, Japan, and [4]Department of Psychiatry, University of Cambridge, Cambridge CB2 0SZ, United Kingdom

Dopamine (DA) is critically involved in processes such as reward anticipation, attention, and decision-making. The present study examined the temporal dynamics of phasic DA transients in the nucleus accumbens core (NAcC) during a visual decisional task based on signal detection theory, using the fluorescent DA sensor dLight1.3b. During the decision-making phase, DA transients in the NAcC encoded real-time outcome expectancy, apparently reflecting the confidence of male rats in their choices. Reward prediction errors (RPEs) emerged following reward delivery and omission and were amplified under conditions of increased uncertainty, produced by either degrading the visual target or introducing interfering distraction. Moreover, DA transients were elicited on both visual signal and no-signal trials. These findings demonstrate that DA fluctuations in the NAcC reflect the RPE that incorporates confidence and levels of uncertainty, emphasizing an involvement of nucleus accumbens DA in adaptive decision-making.

Key words: **attention; decision-making; nucleus accumbens core; reward prediction coding; signal detection**

Significance Statement

This study reveals a novel involvement of the widely studied neurotransmitter dopamine (DA) in coding the confidence of choice responses in well-established visual decision-making in the rat. Reward prediction errors were shown to emerge during manipulations of uncertainty, such as distraction. Similar phasic DA responses in the nucleus accumbens core occurred to both the occurrence and non-occurrence of the discriminative visual stimulus, showing for the first time that such dopaminergic responses are generated to interoceptive as well as exteroceptive discriminative stimuli. These observations thus enhance our understanding of the role of mesoaccumbens DA in perceptual decision-making.

Introduction

Dopamine (DA) is engaged in several behavioral processes but is especially associated with responding to predictive cues associated with reward as well as following reward and punishment omission, in line with the theory of reward prediction error (RPE; Thorpe et al., 1983; Schultz et al., 1997; Schultz, 2016). According to Schultz's RPE hypothesis, DA signaling initially occurs at reward presentation, but during learning, this signal gradually shifts toward predictive cue onset rather than following reward presentation (Chiodo et al., 1980; Steinfels et al., 1983; Schultz and Romo, 1987, 1990). DA RPE transients in response to learning have been well studied. However, the possible role of striatal DA in well-trained, steady-state performance, for example, perceptual decision-making, has been scarcely investigated, despite considerable evidence that striatal DA manipulations affect steady-state performance (Taghzouti et al., 1985; Di Ciano et al., 2001; Giertler et al., 2003; Yun et al., 2004; Stefani and Moghaddam, 2006; Kurti and Matell, 2011; Stopper et al., 2013; du Hoffmann and Nicola, 2014).

Disentangling time-dependent DA fluctuations and their specific functions during signal detection tasks (SDTs) is further complicated by poor spatial and temporal resolution and neurochemical specificity of conventional neurochemical sampling (Nieoullon et al., 1977; Westerink, 1995; Watanabe et al., 1997;

Received Sept. 3, 2025; revised Nov. 26, 2025; accepted Jan. 2, 2026.

Author contributions: L.J.F.W., K.Y., J.W.D., and T.W.R. designed research; L.J.F.W. and C.M. performed research; L.J.F.W. and F.E.A. analyzed data; L.J.F.W., F.E.A., J.W.D., and T.W.R. wrote the paper.

We acknowledge Shionogi & Co. for funding this research. We thank Dr. B.J. Alsiö for his helpful discussions and foundational work, Oliwia Stecko and Merak Chen for their experimental assistance, Dr. Aske Ejdrup for his support during the fiber photometry preprocessing pipeline, and Dr. Armin Lak for his insights into confidence signals in the nucleus accumbens. The experimental work was carried out under a Home Office Project Licence held by Prof. Dr. A. L. Milton.

T.W.R. discloses consultancy with Cambridge Cognition, Supernus Pharmaceuticals, and Platea Biosciences. The authors L.J.F.W.V., C.M., F.E.A., K.Y., and J.W.D. declare no conflicts of interest.

Correspondence should be addressed to Livia J. F. Wilod Versprille at lw621@cam.ac.uk or Jeffrey W. Dalley at jwd20@cam.ac.uk.

This paper contains supplemental material available at: https://doi.org/10.1523/JNEUROSCI.1696-25.2026

https://doi.org/10.1523/JNEUROSCI.1696-25.2026

Copyright © 2026 the authors

Kodama et al., 2002; Phillips et al., 2004; Rossetti and Carboni, 2005; Karakuyu et al., 2007; Howe et al., 2013; Sejnowski et al., 2014; Goedhoop et al., 2023). Consequently, relatively few studies have attempted to measure quasi real-time DA transients during such performance (de Lafuente and Romo, 2011; Sugam et al., 2012; Klanker et al., 2015, 2017).

The present study investigated time-resolved dopaminergic signaling in the nucleus accumbens core (NAcC) during performance of a visual SDT using the fluorescent DA receptor sensor, dLight1.3b. This sensor has successfully been used in vivo to investigate DA transients in the freely behaving rodent, although no previous studies have used a signal detection paradigm designed to measure indices of discriminative sensitivity (d') and bias (β; Patriarchi et al., 2018; Robinson et al., 2019; Condon et al., 2021; Blanco-Pozo et al., 2024). Whereas d' reflects such factors as perceptual accuracy and attention, β indicates motivational tendencies such as perceptual or response bias (e.g., to report signal presence). Notably, the signal detection paradigm utilizes a true no-signal condition requiring top–down attentional control in order to measure perceptual bias or responsivity through measures of correct rejections (CRs) as well as hits, misses, and false alarms (FAs; McGaughy and Sarter, 1995; Turchi et al., 1995; Gill et al., 2000; Apparsundaram et al., 2005; Broussard et al., 2009; Berry et al., 2017). Varying signal durations were utilized to assess DA transients for increasing levels of physical salience, where the no-signal condition controlled for physical salience.

This instrumental visual detection task necessitates higher-order decision-making processes, to assess whether perceptual inputs exceed a sensory threshold for reporting the presence or absence of a visual cue. Moreover, subjects can report the confidence of decisions, reflecting metacognitive evaluation of performance, as reported across species (Foote and Crystal, 2007; Fleming and Dolan, 2012; Kepecs and Mainen, 2012; Fleur et al., 2021). Typically, higher levels of confidence correlate with greater accuracy and influences both decision-making strategies and perceptual sensitivity (d'). Consequently, some studies demonstrated metacognitive sensitivity (meta-d'), which quantifies the relationship between confidence and performance (Maniscalco and Lau, 2012; Massoni et al., 2014; Arnold et al., 2023). Choice confidence may also shape reward anticipation by modulating expectations and adaptive strategies during uncertainty (Lak et al., 2017; Babayan et al., 2018; Kutlu et al., 2021, 2023; Lerner et al., 2021; Hennig et al., 2023).

Hypothetically, multifaceted DA transients may occur during visual signal detection performance. Specifically, an increase in phasic DA release may occur upon (1) cue presence and omission (on specific no-signal trials); (2) during the decision-making aligned to reflect reward expectancy; and (3) reward presentation, with a decrease following nonrewarded incorrect choices.

Materials and Methods

Animals and housing. A total of 16 adult male Sprague Dawley rats (Envigo) housed under a reversed-light cycle and standard cages with wood-chip bedding and cage enrichment (a cardboard tunnel and woodblock) and kept in groups of four until surgeries. Following a post-operative period, the rats were pair-housed. Food restriction was applied when rats reached ~250–300 g bodyweight prior to behavioral experiments and restricted to 90% of their free-feeding bodyweight. There was *ad libitum* water available in the home cage, but not during behavioral experiments. This study has been conducted in accordance with the Animals (Scientific Procedures) Act 1986 Amendment Regulations 2012 (#PA9FBFA9F). Four rats were excluded from the final analysis, with one passing due to surgical complications and three exhibiting insufficient DA transients during the positive control test (see Fig. S1 for representative positive control test).

SDT. The SDT procedures are detailed by Turner and colleagues (Turner et al., 2016, 2017; Turner and Burne, 2016). Briefly, rats received training once or twice daily for 5–7 d a week. First, rats were trained to collect sugar pellets from both food magazines with a nose poke in a magazine triggering the reward. Then, rats were trained to initiate trains by a nose poke in the central port before collecting a pellet in one of the two food magazines. This was followed by signal detection in training Stage 3, where rats had to learn to associate the illumination of a signal light with responding at one food magazine (signal trial) and the absence of the signal cue with responding at the other food magazine (no-signal trial) for a total of 120 trials with 60 signals trials and 60 no-signal trials. Once stable behavior was achieved, variable signal durations (30, 60, and 250 ms) were introduced to increase task difficulty for a minimum of 15 sessions to ensure stable individual performance, before commencing surgery. Which food magazine was assigned to signal trials was counterbalanced across the cohort but remained constant for each individual.

Attentional manipulations: signal uncertainty and distraction. To increase the attentional load and introduce uncertainty, two behavioral manipulations were utilized: the short variable signal duration (short vSD) and visual distractor. The short vSD (10 ms) tested the limit of individual visual perception, increasing task difficulty. The distractor manipulation utilized the house light. This manipulation had interleaved blocks (20 trials each) of standard and distractor trials, where the distractor would start blinking (1 Hz) at the start of each trial until a response was recorded. Retaining the house light's intended use of indicating a time-out period.

Surgical procedures. Subjects were anesthetized to surgically implant an optic fiber (Doric Lenses, 400 µm core diameter 10 mm length) at coordinates (AP +1.5, ML ±1.3, DV −6.3) and infuse the dLight1.3b viral vector (AAV1/2-hSyn1-chl-dLight1.3b-WPRE-bGHpA, Viral Vector Facility ETH Zurich v565-1, 2.5×10^{12} GC/ml) at coordinates (AP +1.5, ML ±1.3, DV −6.1 and −6.5). Viral infusions were administered using a Harvard Micro Syringe Pump Pico Plus and Hamilton 800 series 10 µl syringes, which were connected to a needle through plastic tubing (1 µl virus was infused at 0.1 µl/min for 10 min). Following each infusion, the needle was left in place for 5–10 min to allow for diffusion. Prior to the infusion and following the diffusion, the needle was briefly extended 0.05 mm beyond the target depth to create a "pocket" for the virus. This process was repeated for all coordinates. Subjects were placed in a stereotaxic frame using atraumatic bars while anesthetized with isoflurane (5% for induction and 2–3% for maintenance), and the tooth bar was adjusted for a flat skull. Metal screws and dental cement were used to secure the optic fiber to the skull. The optic fiber implants were protected by a stainless-steel dust cap. Following surgery, rats were single housed and received oral Metacam (meloxicam oral suspension injected into soggy food pellets, Boehringer Ingelheim) for 3 d, before being pair-housed and allowed to recover for the remaining days (≤7 d total).

Fiber photometry recording. FP recordings were performed using Neurophotometrics FP3001 (Neurophotometrics), which uses a blue 470 nm LED and violet 415 nm LED to excite the virally delivered fluorescent targets and detects light emission with a BlackFly camera (FP recordings were interleaved at 40 Hz and 60 mA). Prior to recording, the fiber-optic cables were bleached at full power for a minimum of 30 min. Bonsai (Bonsai Foundation, version 3002) was used to control the Neurophotometrics system, gather FP data, and match behavioral events through external camera recording. The Bonsai camera-recorded behavioral timestamps were then matched to timestamps of behavioral events recorded with KLimbic (Med Associates) through a custom script in RStudio (RStudio, version 2023.06.0, R v4.2.2; R Core Team, 2022).

The Neurophotometrics system was connected to a fiber-optic patch cord [BBP(2)_400/440/LWMJ-0.37_1m_FCM-2xFCM_LAF Branching Bundle Patchcord—Low AutoFluorescence; Doric Lenses], which was attached to a rotary joint (FRJ_1 × 1_PT_400/440/LWMJ-0.37_1m_

FCM_0.10m_FCM Fiberoptic Rotary Joint, pigtailed with 400 µm, NA0.37 fiber, 1 m input, 0.10 m output, optimized for FP, Doric Lenses) and subsequently to a fiber-optic patch cord (MFP_400/440/LWMJ-0.37_0.65m_FC-CM3_LAF Mono Fiberoptic Patchcord—Low AutoFluorescence; Doric Lenses) that was attached to the 400 µm fiber-optic implant.

Prior to connecting the subjects to the cable, both lasers were extinguished to avoid blinding the subjects. The patch cord was then securely attached to the fiber-optic implant, and the rat was placed in the operant chamber. The FP recording was started in Bonsai, and subsequently the 415 nm isosbestic channel was turned on, and after a pause of several seconds, the 470 nm signal channel was turned on. The onset of the traces was visually inspected. The rat was then presented with several (∼3) sucrose pellets to briefly revalidate positive DA signals. Finally, the operant chambers were closed, and the behavioral test was started in the KLimbic program. All Bonsai inputs and behavioral results were monitored to ensure everything was running smoothly. When necessary, the patch cord was tightened during the behavioral task. Once the task finished, the rats were again presented with sucrose pellets to revalidate positive DA signals. The 470 nm signal was then turned off, and finally the 415 nm isosbestic channel was turned off. The Bonsai recording was stopped, and the rat was detached from the patch cord.

Histology. Following the conclusion of behavioral testing, brains were harvested following transcardial perfusion with 0.01 M PBS followed by 10% formalin saline. Brains were submersed in 20% w/v sucrose (Fisher Chemical, S/8560/63) after 24 h. Brains were sliced at 60 µm on a freezing microtome and stored in cryoprotectant solution at −20°C. Cryoprotectant solution was prepared with 30% w/v sucrose, 30% v/v ethylene glycol (Acros Organics, 444230010), 0.547% w/v disodium hydrogen orthophosphate, 0.159% w/v sodium dihydrogen orthophosphate (Signal-Aldrich, 71500), and 0.9% w/v sodium chloride in deionized water at 60°C. Following the dissolution of the abovementioned components 1% w/v polyvinyl pyrrolidone (Acros Organics, 227541000) was added.

Free-floating brain slices were washed three times for 10 min in PBS and blocked (1 h at RT on a shaker) in blocking buffer [BB; 0.01 M PBS, 1% w/v bovine serum albumin (Sigma-Aldrich, A7906) and 0.3% v/v Triton X-100 (Sigma-Aldrich, 3787)]. Followed by incubation (overnight at RT on shaker) with chicken anti-GFP (1:1,000, ab13970 Abcam) and rabbit anti-GFAP (1:1,000, A-85419 Antibodies.com) in BB. Slices were washed three times for 10 min with PBS and incubated (2 h at RT in the dark) with goat anti-chicken (1:2,000, ab175477 Abcam, Alexa Fluor 568) and goat anti-rabbit (1:2,000, A-11008 Thermo Fisher Scientific, Alexa Fluor 488) in BB. Finally, after three 10 min PBS washes, brain slices were mounted on Menzel Gläzer Superfrost Plus (Thermo Fisher Scientific, J1800AMNZ) using FluorSave Reagent (Calbiochem, 345789). Immunohistochemistry visualization and quantification were carried out using a fluorescent microscope (Zeiss AXIO Imager M2 set to 20× magnification) and the software program Visiopharm.

Preprocessing of fiber photometric data. The 470 and 415 nm dLight signal and isosbestic control excitation wavelengths were recorded. The sole integrated preprocessing step from the system was the data scaling. All further processing steps were performed individually by subject and session in Spyder IDE (version 5.4.3; Raybaut, 2009), using Python 3.11.5 (Van Rossum and Drake, 2009) through custom scripts. First, data were loaded and correctly labeled isosbestic and signal. Data were cropped by subject to only include datapoints from the behavioral session as well as datapoints from the 5 s preceding the start of the session and to the 5 s after the completion of the SDT session. Data were then filtered with a zero-phase moving average filter of 1 s in accordance with the method of Sherathiya et al. (2021). The isosbestic control was fitted to the signal as linear decay using least square linear regression. Then the delta F/F and subsequent z-scores were calculated over the whole fitted signal trace, and peristimulus/event time histograms (PSTH) of 6 s were extracted to examine responses to discrete behavioral events over repeated trials. The individual datapoints within each PSTH were rebaselined by means of subtraction of the mean z-score of five baseline trials, inclusive of the current trial.

Frequency filtering. Offline fiber photometry raw data were processed using custom Python 3.11.5 scripts using scipy package (Virtanen et al., 2020) to analyze activity fluctuations across different frequency bands over time. Fiber photometry data were filtered into four different frequency bands using a fourth-order Butterworth bandpass filter at 0.15–0.6, 0.6–2.5 and 2.5–10 Hz, as well as a fourth-order Butterworth low-pass filter with a cutoff frequency of 0.15 Hz. The rationale behind these bands was that Jørgensen et al. (2023) reported slower and faster dynamics on DA-dependent ventral and dorsal striatum, respectively. This processing was done using a forward–backward filtering to avoid the potential frequency-dependent phase shifts (Gustafsson, 1996). Subsequently, data were segmented into epochs of 6 s (−3 to 3 s) with the 0 s centered on the response.

Behavioral analysis. Two-choice tasks commonly report accuracy; however analysis in accordance with the signal detection theory is more appropriate (Tanner and Swets, 1954; Green and Swets, 1966; Stanislaw and Todorov, 1999). First, the number of hits, misses, FAs, and CRs were calculated. A hit was defined as correctly reporting the presence of the visual cue, while a CR was the correct response to the absence of the visual cue. A miss occurred when there was a visual cue and the rat reported that there was no cue, while the FA was the incorrect detection of the visual cue. Thus, both correct responses were rewarded, while their incorrect counterparts prompted a 5 s time-out. Subsequently, the sensitivity and bias were calculated according to the signal detection theory. Sensitivity refers to the capacity of a subject to distinguish between signal and noise trials and was approximated with d' (Eq. 1). Bias refers to the subject's preference for reporting signal or noise (no-signal trials) and was approximated by β (Eq. 2).

$$d' = \Phi^{-1}(p(\text{Hit})) - \Phi^{-1}(p(\text{FA})) = z(p(\text{Hit})) - z(p(\text{FA})).$$

Equation 1: Calculation of sensitivity d', where $\phi^{-1} = z$ and returns a z-score. p(Hit) and p(FA) indicate the probability of making a hit and FA, respectively. The d' is in standard deviation units, where 0 indicates a complete inability to distinguish signal from noise, and larger positive values indicate an increasingly greater ability to distinguish signals from noise. Negative values arise through sampling error or response confusion.

$$\beta = e^{\frac{(\Phi^{-1}(p(\text{Hit})))^2 - (\Phi^{-1}(p(\text{FA})))^2}{2}} = e^{\frac{(z(p(\text{Hit})))^2 - (z(p(\text{FA})))^2}{2}}.$$

Equation 2: Calculation of bias β using the standardized probability of making a hit and FA. A β value of 1 signifies no bias, $\beta < 1$ a bias toward the reporting the signal, and $\beta > 1$ a bias toward reporting its absence.

Data analysis and visualization. Following histological analysis (Fig. 1) and the positive FP control tests, a total of $n = 12$ rats was included in the study. Baseline DA transients were recorded across three consecutive baseline SDT sessions. Transients were averaged by session per trial type before averaging by subject. Subsequently, these values were averaged and used to obtain a representative DA transient for each trial type. To assess differences in DA transients, the signal detection theory trial division was utilized, resulting in distinct DA transients for hits, misses, FAs, and CRs. Additionally, DA transients were grouped according to the signal duration (no-signal, 30 ms, 60 ms, 250 ms, and 1 s). Due to the rapid succession of events within a trial, the results could only be accurately aligned with a singular event. Data were aligned to trial initiation, which coincided with the onset or absence of the signal light, as well as to the recorded nose-poke decision, coinciding with the reward delivery or onset of the house light.

The trial period was divided into three timeframes of interest: (1) trial initiation, (2) decision-making period (≥1 s), and (3) feedback period (Fig. 2*C*). Due to the complexity of the SDT resulting in probable differences in DA transients, various distinctions in the trial type were made

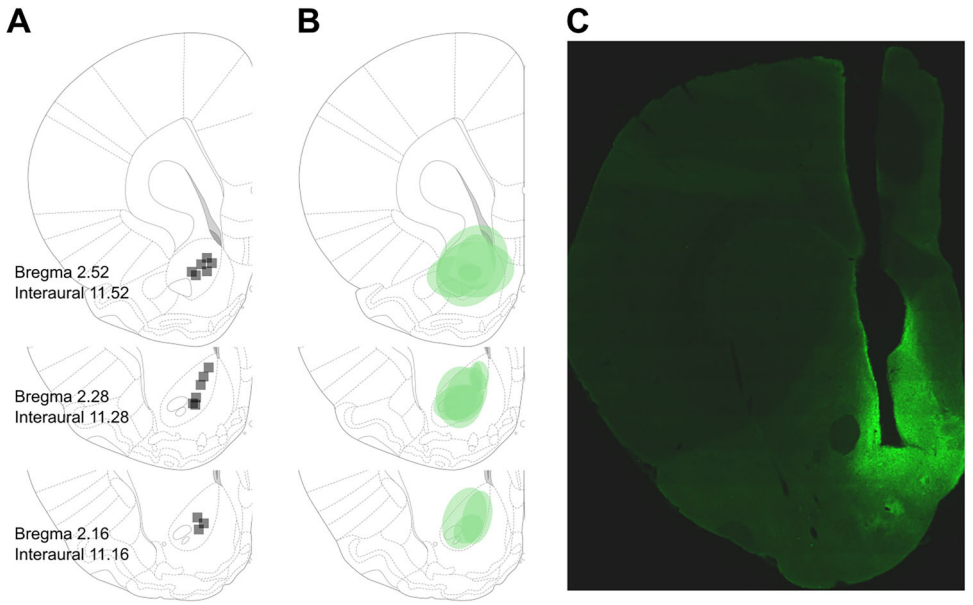

Figure 1. Site of the fiber-optic placement and viral expression of dLight1.3b in the NAcC by subject. ***A***, Fiber-optic placement. ***B***, Viral expression of GFP attached to dLight1.3b. ***C***, Representative example of GFP expression.

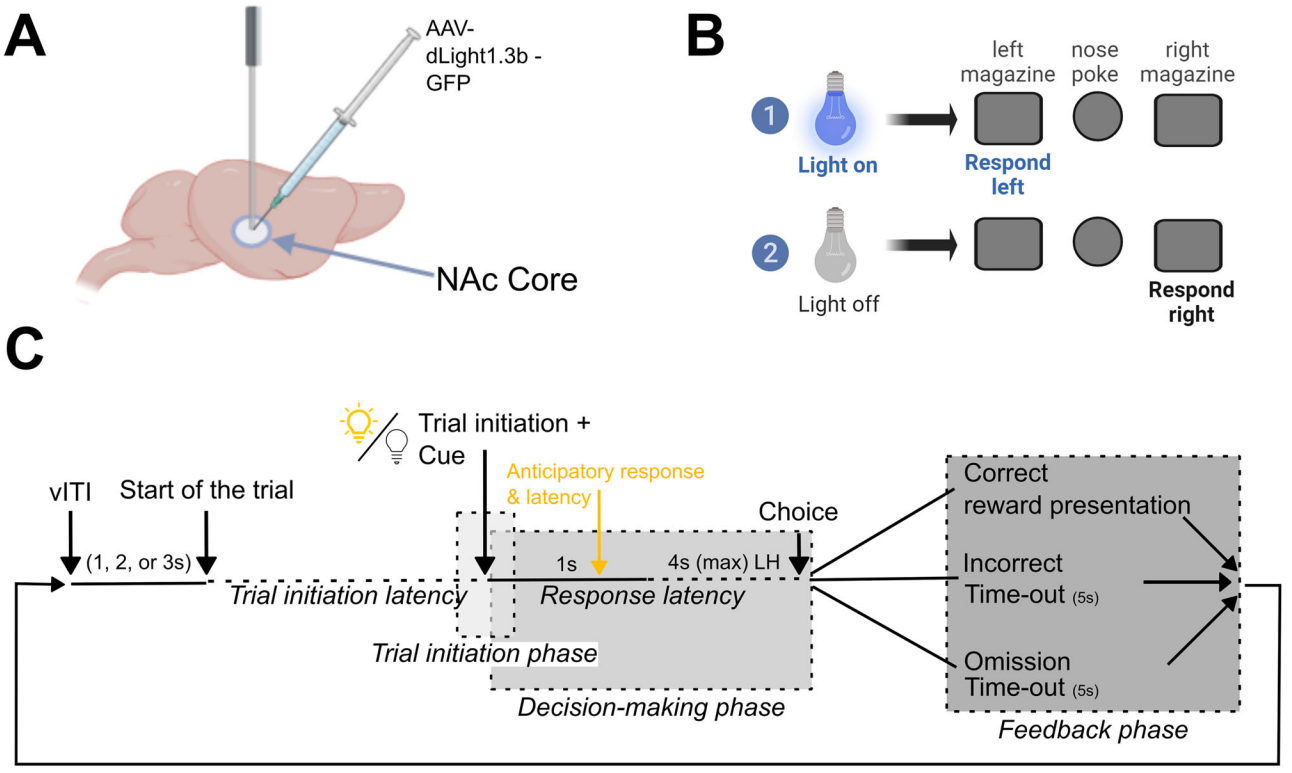

Figure 2. Schematic overview of the experimental and behavioral procedures. ***A***, DA signals were recorded following surgical optic fiber implantation and viral infusion of adeno-associated vector and promotor of dLight1.3b in the NAcC. ***B***, Subjects were trained on the SDT to correctly identify the presence or absence of a visual cue that was triggered by a nose-poke in the central aperture. ***C***, Timeline of a typical trial in the SDT. The SDT trials were self-paced; at the start of the trial the light inside the central nose-poke aperture was illuminated indicating that the subject could initiate a trial through a nose-poke, and the trial initiation latency was recorded. The trial initiation immediately prompted the visual cue directly above the center nose-poke aperture to illuminate or remain off. The interval immediately preceding trial initiation until just after trial initiation was defined as the trial initiation phase. Trial initiation started the decision-making phase, where subjects responded to the respective food magazine (left or right) associated with signal or signal omission. A choice was only recorded after the cue phase (1 s) had elapsed (the response latency was $\geq$1 s); responses made before the end of the 1 s were classified as anticipatory responses with respective choice latency. Following this 1 s period, a choice could be made within the 4 s limited hold (LH) or an omission was recorded and a time-out (onset of the house light for 5 s) commenced. The choice started the feedback phase, where all correct choices were immediately rewarded, and all incorrect choices were immediately punished with a time-out. Subsequently, there was a variable intertrial interval (vITI) of 1, 2, or 3 s before the next trial would begin. LH, limited hold; NAc, nucleus accumbens; vITI, variable intertrial interval. The figure was created in BioRender; Wilod Versprille (2025) https://BioRender.com/b2oe3yx.

based on outcome categories, outcome dependent on the previous outcome, and signal duration. DA transients were compared both visually (qualitatively) and quantitatively through the area under the curve (AUC) values with mixed-model ANOVAs with restricted maximum likelihood. ANOVAs included the following variables: behavioral outcome (within-subject), time frame (within-subject), distractor (within-subject, optional), response speed (within-subject, optional); the rat ID was a random effect to accommodate for repeated measures. *Post-hoc* comparisons were performed where appropriate, and the degrees-of-freedom methods used was the Kenward–Roger method; Tukey's method was used for *p*-value adjustment.

Results

Signal detection performance

Subjects were trained on a visual signal detection paradigm, the SDT (Turner et al., 2016, 2017; Turner and Burne, 2016), prior to surgical intervention and subsequent photometry recordings (Fig. 2). The SDT required rats to repeatedly detect and accurately report the presence of a visual cue. This self-paced instrumental choice task was repeatedly performed to obtain a stable-baseline performance. Repeated testing on the SDT yielded stable and reliable behavior across sessions (Fig. S4); consequently, behavioral and photometry data were averaged over three baseline days. Both the correct detection of the presence of the visual cue (hit) and its absence (CR) resulted in a reward. Analysis based on the signal detection theory outcomes (hits, miss, FAs, and CRs) revealed significant differences in choice outcome (Fig. 3*A*; $F_{(3,56)} = 87.445$; $p < 0.001$) and choice latency (Fig. 3*C*; $F_{(3,162)} = 6.93$; $p < 0.001$). There was a general bias to report the signal (mean ± SEM, $\beta = 0.84 \pm 0.06$) while exhibiting an average sensitivity of $d' = 1.00 \pm 0.13$. The attentional load of the task was enhanced by varying the signal duration of the visual cue (30 ms, 60 ms, 250 ms, and 1 s), with physically more salient signals resulting in higher accuracy compared with shorter signal durations and no-signal trials ($F_{(4,56)} = 26.35$; $p < 0.001$; Fig. S2).

Behavioral manipulations of attentional load (i.e., by either reducing the physical salience of the visual targets through reducing their duration or introducing irrelevant visual stimuli) systematically altered stimulus uncertainty, necessitating greater attentional control (Fig. 3*B*,*D*). Two different manipulations were employed to investigate the influence of uncertainty: the short vSD manipulation introduced a novel, rapid signal duration, while the intradistractor manipulation interspersed blocks of 20 trials with a visual distractor. The manipulations significantly impaired task performance, as evidenced by a reduction in discriminative sensitivity (d', $F_{(3,42)} = 32.38$; $p < 0.001$), but importantly did not affect response bias (β) or response speed (choice latency).

Fiber photometry recordings during visual signal detection performance

To examine DA dynamics during the visual SDT, we transfected dLight1.3b into the NAcC of male Sprague Dawley rats. Three weeks later, dLight1.3b functional expression was investigated by recording DA transients to the noncontingent presentation of sucrose pellets. Subsequently, DA transients were repeatedly recorded during the performance of the visual detection task. There was a high consistency of DA transients across trials, days, and subjects. Subjects were counterbalanced for the signal-associated side and hemisphere, and there was no relationship between DA signal and the recorded hemisphere (left or right), the magazine location (left or right) associated with the responding signal presence, or the hemisphere (ipsilateral or contralateral) connected to the magazine location associated with the signal presence (Fig. S5). Further analysis of the signal into frequency bands revealed that DA activity in the NAcC exhibited slow dynamics (0.15–2.5 Hz) as previously reported by Jørgensen et al. (2023; Fig. S3).

DA transients during SDT performance resemble RPE-like signals

DA transients were measured individually in well-trained rats over the course of three consecutive baseline SDT sessions and averaged by subject according to the trial type (Fig. 4). The omission of a response in either food magazine within the 4 s limited hold were so rare that they were excluded from the analysis. A mixed-effect model examining differences in AUC by outcome and time frame revealed significant main effects of outcome ($F_{(3,264)} = 53.38$; $p < 0.001$) and time frame ($F_{(5,264)} = 29.44$; $p < 0.001$) as well as an outcome × time frame interaction ($F_{(15,264)} = 12.77$; $p < 0.001$). DA consistently spiked at trial initiation irrespective of choice and reward outcome (Fig. 4*A*,*B*). DA elevation centered around the initiation of the trial and discriminative stimulus is the instrumental equivalent of a reward predictive DA signal of a conditioned stimulus. In the feedback phase, DA remained elevated following a correct choice while DA levels decreased below baseline DA levels following an incorrect (unrewarded) response (Fig. 4*A*,*B*). Notably, in the decision-making phase, DA transients were outcome dependent, DA remaining elevated in anticipation of a correct choice, whether correctly reporting a visual target or correctly reporting the absence of the target (i.e., CR). In contrast, in anticipation of an incorrect choice, DA levels began to decrease prior to feedback, again for both signal detection and CRs (Fig. 4*A*,*B*). DA transients thus behave in a manner consistent with RPE theory by reflecting a mismatch between expectation and outcome.

There were no significant differences in DA transients for signal trials compared with no-signal trials. Instead, DA transients were affected by outcome, with hits and CRs as well as misses and FAs exhibiting similar DA signaling profiles. These findings indicate that the absence of a cue produces a discriminative response, reward predictive signal, and RPE signal analogous to that associated with the actual presence of a visual cue.

Signal cues of varying durations were presented, with longer cues (1 s, 250 ms) being more physically salient than shorter cues (30 ms, 60 ms), alongside the no-signal trials without physical salience. The ability to distinguish between short signal cues and no-signal trials differentiated low- and high-attentive subjects. Accuracy was higher for longer signal durations, with rats correctly identifying these signals more frequently. This increased certainty associated with longer signal durations corresponded to elevated DA transients (Fig. 4*C*,*D*), both at trial initiation and throughout the decision-making phase [main effect of signal duration ($F_{(4,319)} = 6.81$; $p < 0.001$) and time frame ($F_{(5,319)} = 29.79$; $p < 0.001$)]. Notably, differences in DA amplitude at trial initiation persisted across correct and incorrect outcomes, while rewarded no-signal trials showed a significant increase in AUC during the feedback phase compared with rewarded 60 and 250 ms trials.

DA transients and reward anticipation

Outcome-dependent differences in DA transients suggest that reward anticipation is dynamically updated throughout the decision-making process, influencing the RPE in real time. To investigate this possibility, DA transients of fast (the 25% trials by subject with the most rapid choice latency; hits 21.2 ± 2.7;

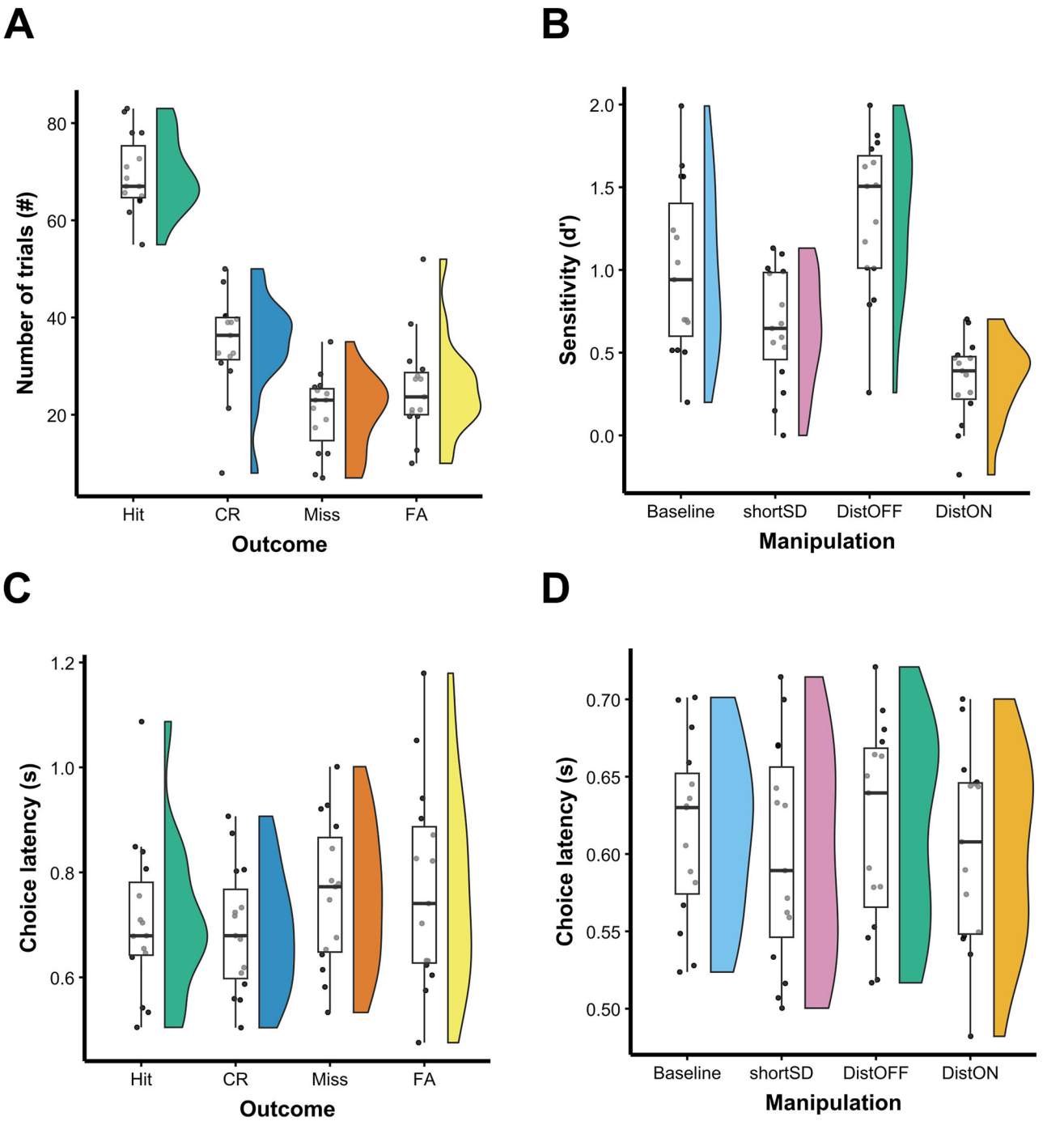

Figure 3. Signal detection performance measures ($n = 15$). ***A***, The average number of signal detection theory outcomes across three baseline sessions by subject. Outcomes include hits, CR, miss, and FA. Mixed linear effects model of signal detection theory outcomes: $F_{(3,56)} = 87.4$; $p < 0.001$. Tukey *post-hoc* tests show significant differences between all outcomes with the exception of misses compared with FA. ***B***, Sensitivity (d') across test conditions, where baseline is averaged for each subject across three sessions, shortSD is the sensitivity during the vSD manipulation, DistOFF is the baseline trials of the visual intradistractor manipulation, and DistON is the interspersed 20 trial blocks with visual distractor. Mixed linear effects model of d': $F_{(3,42)} = 32.38$; $p < 0.001$. Tukey *post-hoc* tests revealed significant differences between all groups: baseline, ShortSD ($t = 3.2$; $p = 0.01$); baseline, DistOFF ($t = -3.1$; $p = 0.02$); baseline, DistON ($t = 6.2$; $p < 0.001$); ShortSD, DistOFF ($t = -6.3$; $p < 0.001$); ShortSD, DistON ($t = 3.0$; $p = 0.02$); DistOFF, DistON ($t = 9.3$; $p < 0.001$). ***C***, Average choice latency for each signal detection theory outcome category across three baseline sessions by subject. Mixed linear effect model of signal detection theory outcomes: $F_{(3,162)} = 6.93$; $p < 0.001$. Tukey *post-hoc* tests revealed significant differences between choice latency of hits, FA ($t = -3.0$; $p = 0.02$); CR, miss ($t = -3.2$; $p = 0.008$); and CR, FA ($t = -3.9$; $p < 0.001$). ***D***, Lack of effect on choice latency across test conditions depicted in ***B***.

CR 13.3 ± 3.7; miss 6.1 ± 1.4; FA 7.5 ± 0.9) and slow responses (the 25% trials by subject with the slowest choice latency; hits 16.8 ± 1.7; CR 10.8 ± 1.9; miss 7.3 ± 1.0; FA 8.6 ± 1.3) were compared, under the assumption that rapid responses reflect heightened decision confidence and increased reward anticipation in accordance with Stolyarova et al. (2019; Fig. 5; Rahnev et al., 2020; Jin et al., 2022; Overhoff et al., 2022). Response speed was found to influence DA transients in an outcome-dependent manner (outcome × choice latency, $F_{(3,\ 511.38)} = 2.32$; $p = 0.07$). Thus, rapid correct responses were associated with increased

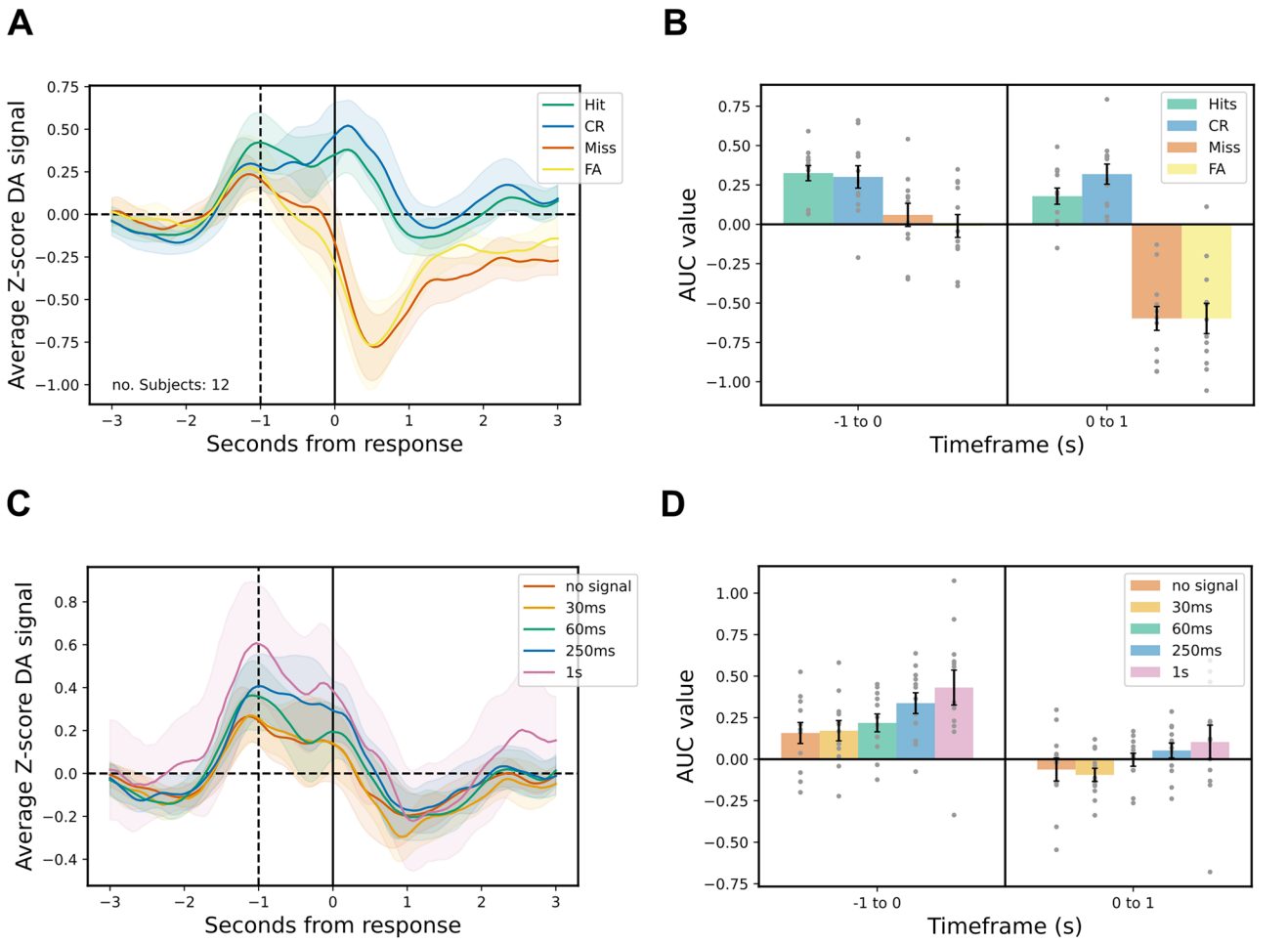

Figure 4. DA transients measured during SDT performance. The left panels (***A***, ***C***) depict the average *Z*-score ± 95% confidence interval for each category and the right panels (***B***, ***D***) depict the AUC (mean ± SEM) for every category, expressed in 1 s timeframes. Fiber photometry (FP) results were averaged across three sessions. Results were aligned to choice and feedback. (***A***) DA transients by response type; (***B***) AUC by response type of −1 to 0 and 0 to 1 s timeframes; (***C***) DA transients by signal duration; (***D***) AUC by signal duration of −1 to 0 and 0 to 1 s timeframes.

DA release and higher peak amplitude (Table S1) at trial initiation and throughout the decision-making phase compared with slower correct responses (time frame × choice latency, $F_{(5,\ 510.87)} = 1.94$; $p = 0.09$). During the feedback phase, slow CRs exhibited elevated DA transients compared with rapid CRs, rapid hits, and slow hits, indicating an increased magnitude of the RPE.

Uncertainty affects DA transients consistent with reward anticipation

We used two behavioral interventions to introduce uncertainty into the task and thereby an increased demand for attentional control (Fig. 6; time frame × behavioral manipulation, $F_{(15,1045)} = 1.69$; $p = 0.048$). The short vSD manipulation did not affect the amplitude of the DA transients at the trial initiation but did affect DA transients throughout the decision-making phase, where DA transients decreased prior to receiving positive and negative feedback (Fig. 6*A*,*B*). Therefore, the outcome-dependent effect seen in the baseline SDT disappeared following this behavioral manipulation. In contrast, the DA transients significantly increased in magnitude following positive feedback and reward presentation, supported by a significant interaction between outcome × time frame ($F_{(15,253)} = 12.72$; $p < 0.001$).

The introduction of a visual distractor affected DA transients in similar fashion, both during distraction and in the interleaved standard SDT trials. In accordance with observations made during the short vSD manipulation, the amplitude of the DA transients increased during positive feedback for both standard and distraction trials (Fig. 6*C*–*F*; outcome × time frame, $F_{(15,517)} = 16.58$; $p < 0.001$; time frame × distractor, $F_{(5,517)} = 2.43$; $p = 0.034$). For CR trials during distraction, there was a diminished DA elevation during the decision-making phase, followed by an enhanced amplitude during the feedback phase, indicative of a RPE. Notably, this DA signaling pattern was specific to the CR trials during distraction and was not observed for Hits during distraction or non-distraction trials. Moreover, during the trial initiation phase for both the standard and distraction trials, the DA amplitude for miss trials was either less pronounced or disappeared entirely, respectively. Thus, reward prediction and errors in reward prediction were dynamically affected by the level of attentional load irrespective of the way it was introduced.

Discussion

Our findings demonstrate that DA transients in the NAcC during performance of a well-trained visual SDT in its decisional phase represent real-time outcome expectancies, whether of success or failure. These transients could be considered to reflect the animals' confidence concerning the outcome, an important component of decision-making (Foote and Crystal, 2007; Kepecs et al.,

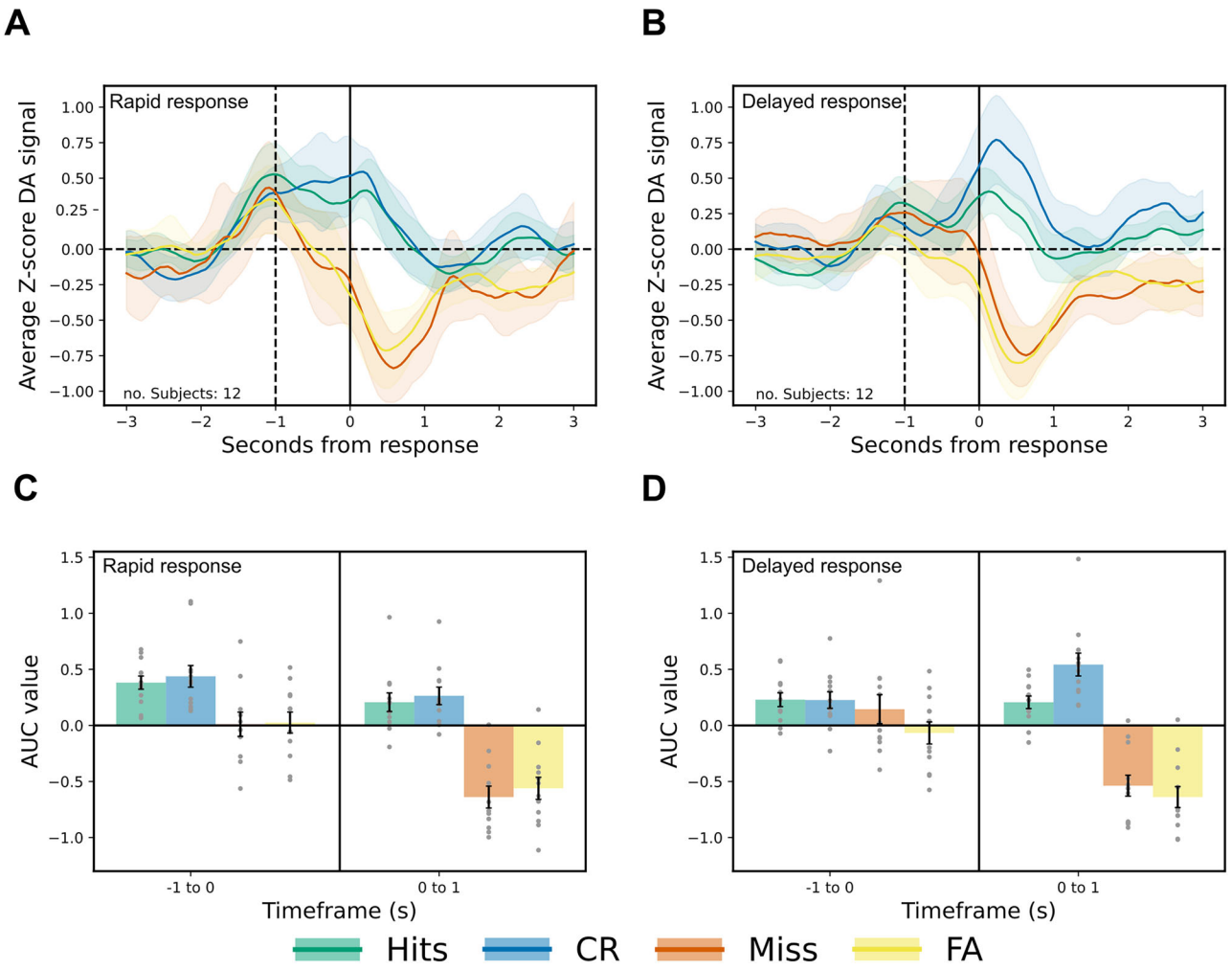

Figure 5. DA transients under low and high confidence. DA transients grouped according to fast and slow anticipatory response times on the (***A***) averaged DA transient by response type for the quartile with most rapid choice latency; (***B***) averaged DA transient by response type for the quartile with the slowest choice latencies; (***C***) AUC by response type of −1 to 0 and 0 to 1 s timeframes for the rapid choices; (***D***) AUC by response type of −1 to 0 and 0 to 1 s timeframes for the slowed choices. FP results were an average of three sessions and depicted as *z*-score ± 95% confidence interval. Results were aligned to choice and feedback.

2008; Yeung and Summerfield, 2012; Arnold et al., 2023; Liebana et al., 2024), as more rapid hits and CRs were associated with greater amplitude DA transients than slower responses. In this well-trained task, RPEs following reward presentation or absence were still evident. However, when task manipulations heightened volatility and increased attentional load—either by shortening the visual signal duration, thereby increasing uncertainty, or by introducing a visual distractor that interfered with signal processing—DA transients during the decision phase became less differentiated. Instead, these manipulations amplified the magnitude of RPEs produced by reward feedback. A further notable discovery was that DA transients were elicited equivalently on visual signal trials and on those trials where no-signal occurred. There was thus no bias in DA transients caused by visual stimulation, and this suggests that the DA responses are most closely associated with the response contingencies associated with these distinct cues rather than their physical salience per se.

DA transients in response to choice feedback reflect an RPE

As hypothesized, the gradual ramping of DA during the discriminative stimulus in this instrumental choice paradigm appears comparable to DA elevations in response to pavlovian conditioned stimuli (Schultz, 2016). Moreover, DA transients occurring in the feedback phase for correct and incorrect responses were consistent with positive and negative RPEs, respectively. Thus, DA transients in this visual detection task are broadly consistent with Schultz's RPE theory, despite occurring during a well-trained self-paced choice paradigm. However, the DA transients observed here more closely followed the RPE two-component response proposed by Schultz (2016), where DA transients act as a utility prediction error signal used for learning, utility, and economic decision-making (Michely et al., 2020; Yun et al., 2020). Additionally, for the task manipulations that heightened volatility and enhanced attentional load, DA transients during the decision-making phase were markedly attenuated. However, those following reward in the feedback phase exhibited greater relative AUC and peak size as compared with no reward trials. Thus, the enhanced uncertainty may well represent a novel learning environment which depends on RPE (Wang et al., 2024). The elevated DA seen in rewarded, uncertain trials, consequent upon the "surprise" of a better-than-expected outcome, further supports the utility of the DA transients in learning and also in decision-making as steady-state performance is re-established. In line with these findings, Li et al. (2023) also reported that dynamic and rapid inter- and intratrial feedback influenced neural reward processing.

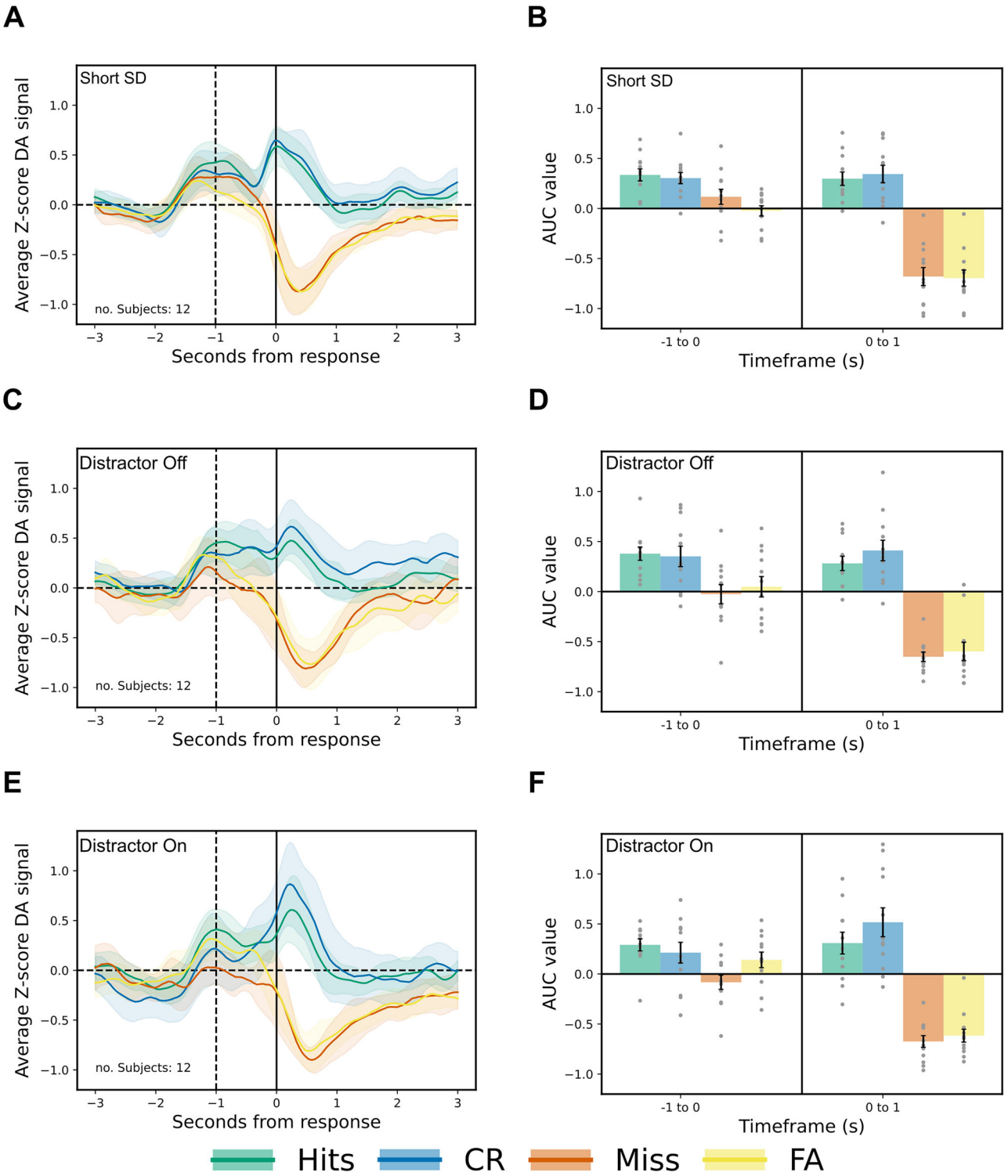

Figure 6. Summary of the effects of increased uncertainty on DA transients during SDT performance. The left panels (***A***, ***C***, ***E***) depict the average *Z*-score ± 95% confidence interval for each category, and the right panels (***B***, ***D***, ***F***) have the AUC (mean ± SEM) for every category in the −1 to 0 and 0 to 1 s timeframes. Results were aligned to choice and feedback. ***A***, ***B***, These panels represent the DA transients following the short vSD manipulation, with 230 trials instead of 170 due to the addition of 30 further no-signal trials and the addition of very rapid signal durations (30× 10 ms). ***C–F***, Represent the DA transients during the intradistractor manipulation, with ***C*** and ***D*** depicting the results during the standard SDT trials and ***E*** and ***F*** depicting the results during the interleaved blocks of trials with visual distractor (house light blinking at 1 Hz from the start of the trial until choice/feedback for blocks of 20 consecutive trials).

Comparable DA transients on signal and no-signal trials

The absence of the visual cue elicited a DA signaling pattern equivalent to that following its presence. Previous studies have demonstrated that DA transients typically occur in response to exteroceptive cues predictive of reward, particularly in pavlovian conditioning tasks (Gan et al., 2010; Nomoto et al., 2010; Kishida et al., 2016; Saunders et al., 2018). These findings are generally interpreted as reflecting reward expectancy. However, the

present instrumental visual detection task necessitates an active choice response to discriminate between signal and no-signal trials, which may engage higher-order decision-making processes.

Our findings reveal that elevated DA transients were associated with decision-making for both hits and CRs, i.e., the detection of the "absence" of the visual signal, while decreasing for misses and FAs, presumably representing attentional failures. Intriguingly, in CR trials, the elevated DA transients were triggered by an interoceptive discriminative stimulus rather than merely occurring simply in reaction to an exteroceptive (visual) cue. This suggests that DA activity arises when a detection threshold fails to be met, highlighting its role in accurately reflecting reward anticipation rather than simply signaling the presence of a sensory cue.

Notably, despite DA transients indicating anticipation of an incorrect choice and subsequent reward omission, subjects did not adjust their decisions. Although this behavior might suggest a dissociation between the neurochemical representation of reward prediction and behavioral adaptation, it could also be explained by the limited, subsecond time available for subjects to monitor and hence modify their choices. While some studies report similar DA signaling patterns in response to both rewarding and aversive cues (Stauffer et al., 2016; Kutlu et al., 2021, 2023; Gershman et al., 2024), no prior work has described this pattern in the context of cue nonoccurrence requiring an active choice.

DA transients driving decision-making reflect real-time reward anticipation and confidence

Especially striking was that DA transients during the decision-making phase were modulated by the "subsequent" outcomes. Trials with correct outcomes exhibited significantly greater DA elevation compared with incorrect trials, particularly during rapid responses. Clinical studies consistently demonstrate that elevated decision confidence is commonly associated with such rapid response times, as demonstrated with the confidence database; a collection of 145 datasets with data from over 8,700 participants (Weidemann and Kahana, 2016; Rahnev et al., 2020; Overhoff et al., 2022). In contrast, no DA elevation was observed on trials with slowed choice latencies, frequently associated with uncertainty and guessing. This suggests that DA transients during decision-making reflect more than classical RPE signaling; they encode a metacognitive belief in choice accuracy or decision confidence and engage DA-dependent processes necessary for effective discrimination.

Several studies support the involvement of metacognitive confidence in decision-making in nonhuman primates and rodents (Foote and Crystal, 2007; Kepecs et al., 2008; Schmack et al., 2021; Starkweather and Uchida, 2021). More precisely, Lak et al. (2017) demonstrated that midbrain DA neurons in macaques reflect both reward size and confidence in decision accuracy, aligning with Bayesian decision-making theory. In a related study, Lak et al. (2020b) showed that mouse choices integrated sensory confidence, past rewards, and learned value, creating a model that bridges signal detection and reinforcement learning principles. Similarly, Kutlu et al. (2021) reported that NAcC DA release in mice reflects the "perceived salience" of stimuli in a discriminative task. However, in the present study, NAcC DA release was enhanced in anticipation of a correct no-signal detection which presumably is devoid of physical salience.

Intriguingly, DA transients for rapid FA and miss trials (both involving active responses) were inconsistent with enhanced reward anticipation, instead declining rapidly during the decision-making phase. These rapid, incorrect responses could reflect impulsive decisions made prematurely before visual processing has concluded; hence, an uninformed guess becomes an informed mistake. Alternatively, rapid incorrect responses may not reflect enhanced confidence, as suggested by Overhoff et al. (2022), who demonstrated a relationship between response speed and self-reported confidence for correct but not for incorrect choices.

Neural circuitry engaged in confidence

Confidence is thought to arise from neural computations integrating sensory input, prior knowledge, and reward prediction. These processes are generally regulated by regions within the frontal cortex such as the medial prefrontal cortex (Lak et al., 2020a) or the orbital frontal cortex (Kepecs et al., 2008). These prefrontal regions affect subcortical regions including the NAcC through top–down signaling pathways; Totah et al. (2013) reported distinct prestimulus activations for correct and incorrect choices in the ventral tegmental area. While the precise role of accumbal DA in confidence remains unclear, it is often expected that such signaling would influence action or choice. However, evidence from Vaghi et al. (2017) suggests that confidence can sometimes operate independently of immediate action.

The observed NAc DA signals may serve as a mechanism that continuously monitors learned, steady-state performance even at asymptote. Hereby, DA signals dynamically evaluate whether behavior should be flexibly updated in response to alterations in reward expectation as well as reward feedback. Rather than solely guide immediate action, this signaling may modulate longer-term decision strategies or encode belief states that inform future behavior as proposed by Lak et al. (2017). The frontal cortex likely plays a critical role in integrating signals projecting from the NAcC, as well as possibly other DA-dependent striatal regions such as the NAc shell and dorsal striatum and modifying behavior appropriately. How cortical regions involved in metacognition influence DA signals in the NAcC requires clarification. Specifically, future studies should investigate whether these signals integrate confidence with learned expectations and executive processes such as behavioral flexibility, task-switching, and attention. Moreover, these studies could address the distinct contributions of subcortical regions and the role of other neuromodulators, such as acetylcholine and noradrenaline (Aston-Jones and Cohen, 2005; Kehagia et al., 2010; Sarter and Paolone, 2011). Additionally, including females is merited in future studies, although studies to date indicate quantitative not qualitative sex differences (Cummings et al., 2014), e.g., with reward-related NAc fMRI response, a proxy for RPE, Joue et al. (2022) demonstrated enhanced RPE in women.

Conclusion

These findings highlight the nuanced role of DA fluctuations in the NAcC, demonstrating their critical function in regulating decision-making processes. By linking real-time reward evaluation to confidence and uncertainty, this work underscores the neurochemical complexity underlying adaptive behavior and provides a foundation for future studies exploring DA's role in perceptual and executive functions.

References

Apparsundaram S, Martinez V, Parikh V, Kozak R, Sarter M (2005) Increased capacity and density of choline transporters situated in synaptic membranes of the right medial prefrontal cortex of attentional task-performing rats. J Neurosci 25:3851–3856.

Arnold DH, Johnston A, Adie J, Yarrow K (2023) On why we lack confidence in some signal-detection-based analyses of confidence. Conscious Cogn 113:103532.
Aston-Jones G, Cohen JD (2005) An integrative theory of locus coeruleus-norepinephrine function: adaptive gain and optimal performance. Annu Rev Neurosci 28:403–450.
Babayan BM, Uchida N, Gershman SJ (2018) Belief state representation in the dopamine system. Nat Commun 9:1891.
Berry AS, Sarter M, Lustig C (2017) Distinct frontoparietal networks underlying attentional effort and cognitive control. J Cogn Neurosci 29:1212–1225.
Blanco-Pozo M, Akam T, Walton ME (2024) Dopamine-independent effect of rewards on choices through hidden-state inference. Nat Neurosci 27:286–297.
Broussard JI, Karelina K, Sarter M, Givens B (2009) Cholinergic optimization of cue-evoked parietal activity during challenged attentional performance. Eur J Neurosci 29:1711–1722.
Chiodo LA, Antelman SM, Caggiula AR, Lineberry CG (1980) Sensory stimuli alter the discharge rate of dopamine (DA) neurons: evidence for two functional types of DA cells in the substantia nigra. Brain Res 189:544549.
Condon AF, Robinson BG, Asad N, Dore TM, Tian L, Williams JT (2021) The residence of synaptically released dopamine on D2 autoreceptors. Cell Rep 36:109465.
Cummings JA, Jagannathan L, Jackson LR, Becker JB (2014) Sex differences in the effects of estradiol in the nucleus accumbens and striatum on the response to cocaine: neurochemistry and behavior. Drug Alcohol Depend 135:22–28.
de Lafuente V, Romo R (2011) Dopamine neurons code subjective sensory experience and uncertainty of perceptual decisions. Proc Natl Acad Sci U S A 108:19767–19771.
Di Ciano P, Cardinal RN, Cowell RA, Little SJ, Everitt BJ (2001) Differential involvement of NMDA, AMPA/kainate, and dopamine receptors in the nucleus accumbens core in the acquisition and performance of pavlovian approach behavior. J Neurosci 21:9471–9477.
du Hoffmann J, Nicola SM (2014) Dopamine invigorates reward seeking by promoting cue-evoked excitation in the nucleus accumbens. J Neurosci 34:14349–14364.
Fleming SM, Dolan RJ (2012) The neural basis of metacognitive ability. Philos Trans R Soc Lond B Biol Sci 367:1338–1349.
Fleur DS, Bredeweg B, van den Bos W (2021) Metacognition: ideas and insights from neuro- and educational sciences. NPJ Sci Learn 6:13.
Foote AL, Crystal JD (2007) Metacognition in the rat. Curr Biol 17:551–555.
Gan JO, Walton ME, Phillips PEM (2010) Dissociable cost and benefit encoding of future rewards by mesolimbic dopamine. Nat Neurosci 13:25–27.
Gershman SJ, Assad JA, Datta SR, Linderman SW, Sabatini BL, Uchida N, Wilbrecht L (2024) Explaining dopamine through prediction errors and beyond. Nat Neurosci 27:1645–1655.
Giertler C, Bohn I, Hauber W (2003) The rat nucleus accumbens is involved in guiding of instrumental responses by stimuli predicting reward magnitude. Eur J Neurosci 18:1993–1996.
Gill TM, Sarter M, Givens B (2000) Sustained visual attention performance-associated prefrontal neuronal activity: evidence for cholinergic modulation. J Neurosci 20:4745–4757.
Goedhoop J, Arbab T, Willuhn I (2023) Anticipation of appetitive operant action induces sustained dopamine release in the nucleus accumbens. J Neurosci 43:3922–3932.
Green DM, Swets JA (1966) *Signal detection theory and psychophysics*. Oxford: John Wiley.
Gustafsson F (1996) Determining the initial states in forward-backward filtering. IEEE Trans Signal Process 44:988–992.
Hennig JA, Romero Pinto SA, Yamaguchi T, Linderman SW, Uchida N, Gershman SJ (2023) Emergence of belief-like representations through reinforcement learning. PLoS Comput Biol 19:e1011067.
Howe MW, Tierney PL, Sandberg SG, Phillips PEM, Graybiel AM (2013) Prolonged dopamine signalling in striatum signals proximity and value of distant rewards. Nature 500:575–579.
Jin S, Verhaeghen P, Rahnev D (2022) Across-subject correlation between confidence and accuracy: a meta-analysis of the confidence database. Psychon Bull Rev 29:1405–1413.
Jørgensen SH, Ejdrup AL, Lycas MD, Posselt LP, Madsen KL, Tian L, Dreyer JK, Herborg F, Sørensen AT, Gether U (2023) Behavioral encoding across timescales by region-specific dopamine dynamics. Proc Natl Acad Sci U S A 120:e2215230120.
Joue G, Chakroun K, Bayer J, Gläscher J, Zhang L, Fuss J, Hennies N, Sommer T (2022) Sex differences and exogenous estrogen influence learning and brain responses to prediction errors. Cereb Cortex 32:2022–2036.
Karakuyu D, Herold C, Güntürkün O, Diekamp B (2007) Differential increase of extracellular dopamine and serotonin in the 'prefrontal cortex' and striatum of pigeons during working memory. Eur J Neurosci 26:2293–2302.
Kehagia AA, Murray GK, Robbins TW (2010) Learning and cognitive flexibility: frontostriatal function and monoaminergic modulation. Curr Opin Neurobiol 20:199–204.
Kepecs A, Mainen ZF (2012) A computational framework for the study of confidence in humans and animals. Philos Trans R Soc Lond B Biol Sci 367:1322–1337.
Kepecs A, Uchida N, Zariwala HA, Mainen ZF (2008) Neural correlates, computation and behavioural impact of decision confidence. Nature 455:227–231.
Kishida KT, Saez I, Lohrenz T, Witcher MR, Laxton AW, Tatter SB, White JP, Ellis TL, Phillips PEM, Montague PR (2016) Subsecond dopamine fluctuations in human striatum encode superposed error signals about actual and counterfactual reward. Proc Natl Acad Sci U S A 113:200–205.
Klanker M, Sandberg T, Joosten R, Willuhn I, Feenstra M, Denys D (2015) Phasic dopamine release induced by positive feedback predicts individual differences in reversal learning. Neurobiol Learn Mem 125:135–145.
Klanker M, Fellinger L, Feenstra M, Willuhn I, Denys D (2017) Regionally distinct phasic dopamine release patterns in the striatum during reversal learning. Neuroscience 345:110–123.
Kodama T, Hikosaka K, Watanabe M (2002) Differential changes in glutamate concentration in the primate prefrontal cortex during spatial delayed alternation and sensory-guided tasks. Exp Brain Res 145:133–141.
Kurti AN, Matell MS (2011) Nucleus accumbens dopamine modulates response rate but not response timing in an interval timing task. Behav Neurosci 125:215–225.
Kutlu MG, Zachry JE, Melugin PR, Cajigas SA, Chevee MF, Kelly SJ, Kutlu B, Tian L, Siciliano CA, Calipari ES (2021) Dopamine release in the nucleus accumbens core signals perceived saliency. Curr Biol 31:4748–4761.e8.
Kutlu MG, Tat J, Christensen BA, Zachry JE, Calipari ES (2023) Dopamine release at the time of a predicted aversive outcome causally controls the trajectory and expression of conditioned behavior. Cell Rep 42:112948.
Lak A, Nomoto K, Keramati M, Sakagami M, Kepecs A (2017) Midbrain dopamine neurons signal belief in choice accuracy during a perceptual decision. Curr Biol 27:821–832.
Lak A, et al. (2020a) Reinforcement biases subsequent perceptual decisions when confidence is low, a widespread behavioral phenomenon (Salinas E, Frank MJ, Salinas E, Brody CD, Ding L, eds). Elife 9:e49834.
Lak A, Okun M, Moss MM, Gurnani H, Farrell K, Wells MJ, Reddy CB, Kepecs A, Harris KD, Carandini M (2020b) Dopaminergic and prefrontal basis of learning from sensory confidence and reward value. Neuron 105:700–711.e6.
Lerner TN, Holloway AL, Seiler JL (2021) Dopamine, updated: reward prediction error and beyond. Curr Opin Neurobiol 67:123–130.
Li Z, Duan R, Guo Y, Li P, Warren CM (2023) Distinct influence of inter- versus intra-trial feedback on the brain response to subsequent feedback: evidence from event-related potentials. Biol Psychol 181:108596.
Liebana S, Fritsche M, Lak A (2024) Dopaminergic computations for perceptual decisions. Curr Opin Behav Sci 60:101458.
Maniscalco B, Lau H (2012) A signal detection theoretic approach for estimating metacognitive sensitivity from confidence ratings. Conscious Cogn 21:422–430.
Massoni S, Gajdos T, Vergnaud J-C (2014) Confidence measurement in the light of signal detection theory. Front Psychol 5:1455.
McGaughy J, Sarter M (1995) Behavioral vigilance in rats: task validation and effects of age, amphetamine, and benzodiazepine receptor ligands. Psychopharmacology 117:340–357.
Michely J, Viswanathan S, Hauser TU, Delker L, Dolan RJ, Grefkes C (2020) The role of dopamine in dynamic effort-reward integration. Neuropsychopharmacology 45:1448–1453.
Nieoullon A, Cheramy A, Glowinski J (1977) Release of dopamine in vivo from cat substantia nigra. Nature 266:375–377.
Nomoto K, Schultz W, Watanabe T, Sakagami M (2010) Temporally extended dopamine responses to perceptually demanding reward-predictive stimuli. J Neurosci 30:10692–10702.

Overhoff H, Ko YH, Fink GR, Stahl J, Weiss PH, Bode S, Niessen E (2022) The relationship between response dynamics and the formation of confidence varies across the lifespan. Front Aging Neurosci 14:969074.
Patriarchi T, et al. (2018) Ultrafast neuronal imaging of dopamine dynamics with designed genetically encoded sensors. Science 360:eaat4422.
Phillips AG, Ahn S, Floresco SB (2004) Magnitude of dopamine release in medial prefrontal cortex predicts accuracy of memory on a delayed response task. J Neurosci 24:547–553.
Rahnev D, et al. (2020) The confidence database. Nat Hum Behav 4:317–325.
Raybaut P (2009) Spyder-documentation. Available at: pythonhosted.org
R Core Team (2022) R: a language and environment for statistical computing. R Foundation for Statistical Computing, Vienna, Austria. Available at: http://www.R-project.org
Robinson JE, Coughlin GM, Hori AM, Cho JR, Mackey ED, Turan Z, Patriarchi T, Tian L, Gradinaru V (2019) Optical dopamine monitoring with dLight1 reveals mesolimbic phenotypes in a mouse model of neurofibromatosis type 1. Elife 8:e48983.
Rossetti ZL, Carboni S (2005) Noradrenaline and dopamine elevations in the rat prefrontal cortex in spatial working memory. J Neurosci 25:2322–2329.
Sarter M, Paolone G (2011) Deficits in attentional control: cholinergic mechanisms and circuitry-based treatment approaches. Behav Neurosci 125: 825–835.
Saunders BT, Richard JM, Margolis EB, Janak PH (2018) Dopamine neurons create Pavlovian conditioned stimuli with circuit-defined motivational properties. Nat Neurosci 21:1072–1083.
Schmack K, Bosc M, Ott T, Sturgill JF, Kepecs A (2021) Striatal dopamine mediates hallucination-like perception in mice. Science 372:eabf4740.
Schultz W (2016) Dopamine reward prediction-error signalling: a two-component response. Nat Rev Neurosci 17:183–195.
Schultz W, Romo R (1987) Responses of nigrostriatal dopamine neurons to high-intensity somatosensory stimulation in the anesthetized monkey. J Neurophysiol 57:201–217.
Schultz W, Romo R (1990) Dopamine neurons of the monkey midbrain: contingencies of responses to stimuli eliciting immediate behavioral reactions. J Neurophysiol 63:607–624.
Schultz W, Dayan P, Montague PR (1997) A neural substrate of prediction and reward. Science 275:1593–1599.
Sejnowski TJ, Churchland PS, Movshon JA (2014) Putting big data to good use in neuroscience. Nat Neurosci 17:1440–1441.
Sherathiya VN, Schaid MD, Seiler JL, Lopez GC, Lerner TN (2021) GuPPy, a Python toolbox for the analysis of fiber photometry data. Sci Rep 11: 24212.
Stanislaw H, Todorov N (1999) Calculation of signal detection theory measures. Behav Res Methods Instrum Comput 31:137–149.
Starkweather CK, Uchida N (2021) Dopamine signals as temporal difference errors: recent advances. Curr Opin Neurobiol 67:95–105.
Stauffer WR, Lak A, Kobayashi S, Schultz W (2016) Components and characteristics of the dopamine reward utility signal. J Comp Neurol 524: 1699–1711.
Stefani MR, Moghaddam B (2006) Rule learning and reward contingency are associated with dissociable patterns of dopamine activation in the rat prefrontal cortex, nucleus accumbens, and dorsal striatum. J Neurosci 26: 8810–8818.
Steinfels GF, Heym J, Strecker RE, Jacobs BL (1983) Behavioral correlates of dopaminergic unit activity in freely moving cats. Brain Res 258:217–228.
Stolyarova A, Rakhshan M, Hart EE, O'Dell TJ, Peters MAK, Lau H, Soltani A, Izquierdo A (2019) Contributions of anterior cingulate cortex and basolateral amygdala to decision confidence and learning under uncertainty. Nat Commun 10:4704.
Stopper CM, Khayambashi S, Floresco SB (2013) Receptor-specific modulation of risk-based decision making by nucleus accumbens dopamine. Neuropsychopharmacology 38:715–728.
Sugam JA, Day JJ, Wightman RM, Carelli RM (2012) Phasic nucleus accumbens dopamine encodes risk-based decision-making behavior. Biol Psychiatry 71:199–205.
Taghzouti K, Louilot A, Herman JP, Le Moal M, Simon H (1985) Alternation behavior, spatial discrimination, and reversal disturbances following 6-hydroxydopamine lesions in the nucleus accumbens of the rat. Behav Neural Biol 44:354–363.
Tanner WP Jr, Swets JA (1954) A decision-making theory of visual detection. Psychol Rev 61:401–409.
Thorpe SJ, Rolls ET, Maddison S (1983) The orbitofrontal cortex: neuronal activity in the behaving monkey. Exp Brain Res 49:93–115.
Totah NKB, Kim Y, Moghaddam B (2013) Distinct prestimulus and poststimulus activation of VTA neurons correlates with stimulus detection. J Neurophysiol 110:75–85.
Turchi J, Holley LA, Sarter M (1995) Effects of nicotinic acetylcholine receptor ligands on behavioral vigilance in rats. Psychopharmacology 118:195–205.
Turner KM, Burne THJ (2016) Improvement of attention with amphetamine in low- and high-performing rats. Psychopharmacology 233:3383–3394.
Turner KM, Peak J, Burne THJ (2016) Measuring attention in rodents: comparison of a modified signal detection task and the 5-choice serial reaction time task. Front Behav Neurosci 9:370.
Turner KM, Peak J, Burne THJ (2017) Baseline-dependent effects of amphetamine on attention are associated with striatal dopamine metabolism. Sci Rep 7:297.
Vaghi MM, Luyckx F, Sule A, Fineberg NA, Robbins TW, De Martino B (2017) Compulsivity reveals a novel dissociation between action and confidence. Neuron 96:348–354.e4.
Van Rossum G, Drake FL Jr (2009) Python 3 reference manual, version 3.7.3. Scotts Valley: CreateSpace.
Virtanen P, et al. (2020) Scipy 1.0: fundamental algorithms for scientific computing in Python. Nat Methods 17:261–272.
Wang Y, Lak A, Manohar SG, Bogacz R (2024) Dopamine encoding of novelty facilitates efficient uncertainty-driven exploration. PLoS Comput Biol 20:e1011516.
Watanabe M, Kodama T, Hikosaka K (1997) Increase of extracellular dopamine in primate prefrontal cortex during a working memory task. J Neurophysiol 78:2795–2798.
Weidemann CT, Kahana MJ (2016) Assessing recognition memory using confidence ratings and response times. R Soc Open Sci 3:150670.
Westerink BH (1995) Brain microdialysis and its application for the study of animal behaviour. Behav Brain Res 70:103–124.
Yeung N, Summerfield C (2012) Metacognition in human decision-making: confidence and error monitoring. Philos Trans R Soc Lond B Biol Sci 367:1310–1321.
Yun IA, Nicola SM, Fields HL (2004) Contrasting effects of dopamine and glutamate receptor antagonist injection in the nucleus accumbens suggest a neural mechanism underlying cue-evoked goal-directed behavior. Eur J Neurosci 20:249–263.
Yun M, Kawai T, Nejime M, Yamada H, Matsumoto M (2020) Signal dynamics of midbrain dopamine neurons during economic decision-making in monkeys. Sci Adv 6:eaba4962.